Heat and mass transfer characteristics of a nanofluid flow past a vertical slender permeable cylinder

Hanumesh Vaidya

Department of Mathematics, SSA Government First Grade College (Autonomous), Ballari-583 101, Karnataka, India.

E-mail: hanumeshvaidya@gmail.com

Abstract: This paper presents the mathematical model for analyzing the nanofluid flow over a vertical porous slender cylinder. Heat and mass transfer characteristics are considered. Flow is driven exclusively by linearly stretching the cylinder and the nanofluid model is of two phase fluid where the nanoparticles move arbitrarily and increase the energy exchange rates therefore consolidating the impacts of Brownian movement and thermophoresis. The governing cylindrical equations are transformed into coupled ordinary differential equations using suitable transformation and are solved numerically via Keller box method. The impact of physical parameters on the velocity, temperature and concentration profiles are presented graphically and analyzed. To validate the numerical method, comparisons are made with the available results in the literature for some special cases and the results are found to be in excellent agreement. The analysis reveals many interesting behaviors that warrant further study on the axi-symmetric flow phenomena especially the nanofluid past a vertical slender cylinder.

Keywords: Slender cylinder; Porous media; Nanofluid; Brownian motion, Thermophoresis; Keller box method.

1. INTRODUCTION

In recent years, significant consideration has been paid to the investigation of nanofluids in light of its applications in communication, computing technologies, optical devices, lasers, high-power scientific measurement, medicine and material synthesis. The mechanical business has grasped a few approaches to enhance the effectiveness of the heat exchange, in particular, usage of broadened surfaces, use of vibration to the heat exchange surfaces, and use of microchannel. The thermal conductivity of a liquid plays an indispensable part during the time spent enhancing the proficiency of the heat exchange. Most ordinarily utilized heat transfer liquids are water, ethylene glycol, and motor oil which are with generally low thermal conductivities in correlation with solids. The expansion of little amount of strong particles with high thermal conductivity to the liquid (ethylene glycol+ water, water + propylene glycol and so on.,) brings about an expansion in the thermal conductivity of a liquid. Choi [1] used one of the leading techniques and proposed an imaginative new class of heat exchange liquids which can be outlined by suspending metallic nanoparticles in customary heat exchange liquids and watched that one of the advantages of nanofluids is an expressive diminishment in heat transfer pumping power and also he coined the term ‘‘nanofluid” which are relatively new and high class of fluids having suspension of nano-sized metallic or nonmetallic particles (1 - 100 nm) with the base fluid. Buongiorno [2] explains that the nanoparticle absolute velocity can be viewed as the sum of the base fluid velocity and the relative velocity and claimed that, for laminar flow, Brownian diffusion and thermophoretic diffusion have a prominent effect. Further, he modeled the governing equations for the nanofluid flow and dissected the conceivable impact of seven slip components on heat transfer enhancement and presumed that exclusive Brownian movement and thermophoresis are the vital slip systems. Several researchers have worked on the

behavior of nanofluid flow by considering Buongiorno model (Shehzada et al. [3], Sheikholeslami et al. [4], Prasad et al. [5-6]).

All the above analysts confined their examinations to flow and heat exchange over an even/ horizontal plate. The vast majority of the issues emerging in innovative industry, in light of blended convection flow over a heated vertical sheet is of significant intrigue and is test to physicists, designers and Mathematicians. The convective stream over a vertical slender cylender has picked up energy on account of its broad applications in numerous branches of science and innovation, for example, the atomic reactors cooled amid crisis shutdown, electronic gadgets cooled by fans, heat exchangers put in a low speed condition, sunlight based focal collectors presented to wind ebbs and flows, soften turning procedure, wire and fiber drawing, and so forth. Stream over chambers is thought to be two-dimensional if the body range is vast contrasted with the limit layer thickness. For a thin cylinder, the range of the chamber might be of an indistinguishable request from the limit layer thickness. Along these lines the stream might be considered as axisymmetric rather than two-dimensional. In perspective of this, Wang [7] considered the flow of a fluid at a stretching cylinder in an ambient fluid at rest. Numerous investigators have contemplated the liquid stream, heat and mass exchange under various physical circumstances (Ishak and Nazar [8], Bachok and Ishak [9], Chamkha et al [10], Ishak [11], Prasad et al [12] and Vajravelu et al. [13]).

The physical phenomena in which the distinction between the surface temperature and the free stream temperature in particular $(T_w - T_\infty)$ is obviously extensive. The discoveries for such a physical phenomenon will have an unequivocal bearing on the plastic, texture and polymer ventures. Thus, it is intriguing to contemplate the impacts of thermal buoyancy and the Prandtl number. Thermal buoyancy is accepted to be of central significance to the liquid stream what more, characteristics around bluff obstacles. Critical control of the boundary layer can be accomplished through controlled heating or cooling of the body as for the isothermal free stream. In numerous functional circumstances the material moves in a quiet liquid with the liquid velocity incited by the movement of the strong material and by the thermal buoyancy. Along these lines the subsequent velocity and the temperature fields are dictated by these two instruments. It is outstanding that the buoyancy force originating from the heating or cooling of the nonstop stretching sheet change the velocity and the temperature fields and consequently, the heat exchange attributes of the assembling forms. Be that as it may, the buoyancy force impacts were not considered in the up to specified investigations. The issue of blended convection boundary layer velocity of a uniform stream past an isothermal vertical circular cylinder has been talked about by Mahmood and Merkin [14] when the lightness powers help or restrict the advancement of boundary layer with endorsed wall temperature. Ganesan and Loganathan [15] dissected the issue of radiation consequences with the expectation of complimentary convection velocity past a impulsively started semi-infinite vertical cylinder within the sight of mass exchange. Bachok and Ishak [16] examined the impulsively started stream along a porous vertical cylinder with endorsed surface heat flux. Rani and Devaraj [17] examined the flow and heat transfer of a unsteady flow over a semi-infinite vertical cylinder considering temperature oscillation.

To the best of authors' learning, very little consideration has been paid to comprehend the impacts of nanofluid parameters on the free convective stream of a nanofluid over a vertical permeable slender cylinder. Consequently, the issue considered is in contrast to the work of Vajravelu et al. [18], in considering the impacts of base-liquid and expecting it to be a two-segment non-homogeneous equilibrium demonstrate with Brownian dissemination and thermophoresis alongside buoyancy impacts because of temperature distinction and in addition nanoparticles species dispersion. For this situation, the governing equations contain the transverse curvature term which firmly impacts the convective flow, heat and mass exchange fields. The coupled non-linear ordinary differential equations overseeing the issue are changed to an arrangement of coupled non-direct common differential equations. The

changed equations are understood numerically through a second request limited distinction plot known as the Keller-box strategy (See Vajravelu and Prasad [19]). The impacts of pertinent parameters on the velocity, temperature, nanoparticles concentration fields are displayed graphically and the numerical qualities for the local skin contact coefficient, the local Nusselt number and the local Sherwood number are recorded in Table I. It is expected that the outcomes acquired from the present examination will give valuable data to applications and will likewise fill in as a supplement to past investigations.

2. Mathematical formulation

Consider a steady nanofluid flow past a permeable vertical slender cylinder of constant radius *a*. The surface of the vertical slender cylinder is assumed to have linear stretching velocity, prescribed surface temperature and the prescribed species diffusion, which are of the following forms

$$U_w(x) = b\left(x/l\right),$$

$$T_w(x) = T_\infty + T_0\left(x/l\right),$$

$$C_w(x) = C_\infty + C_0\left(x/l\right)$$

Here, b, l are the stretching rate and the reference length; T_0 and C_0 are constants. The problem statements for nanofluids are

$$ru_x + \left(rv\right)_r = 0, \tag{1}$$

$$uu_x + \mathrm{v}u_r = \nu_f\left(u_{rr} + \frac{1}{r}u_r\right) \pm \frac{g\beta\left(T - T_\infty\right)}{\rho_f} + \frac{g\beta^*(C - C_\infty)}{\rho_f} - \frac{\nu_f u}{K'}, \tag{2}$$

$$uT_x + \mathrm{v}T_r = \alpha\left[T_{rr} + \frac{1}{r}T_r\right] + \tau\left[D_B\left(C_rT_r\right) + \frac{D_T}{T_\infty}\left(T_r\right)^2\right], \tag{3}$$

$$uC_x + \mathrm{v}C_r = D_B\left[C_{rr} + \frac{1}{r}C_r\right] + \frac{D_T}{T_\infty}\left[T_{rr} + \frac{1}{r}T_r\right], \tag{4}$$

where (u, v) are the velocity components measured along the (x, r) directions of the slender cylinder. Here, D_B is Brownian motion diffusion coefficient, D_T is thermophoresis diffusion coefficient and in this paper, the temperature dependent liquid properties, to be specific, fluid viscosity, fluid thermal conductivity and fluid species diffusivity are thought to be elements of temperature and the nanoparticles species diffusion. The boundary conditions for the physical problem under consideration are given by

$$u = U_w, \quad \mathrm{v} = 0, \quad T = T_w, \quad C = C_w \quad \text{at} \quad r = a,$$
$$u \to 0, \; T \to T_\infty, \; C \to C_\infty \quad \text{as} \quad r \to \infty. \tag{5}$$

It is convenient to reduce the number of equations from four to three as well as to transform them in to dimensionless form. Introducing the dimensionless functions f, θ and ϕ and the similarity variable η as (See Praasad et al. [20]) :

$$\psi = \left(\nu_f x U_w\right)^{\frac{1}{2}} a\, f(\eta), \quad \theta(\eta) = \frac{T - T_\infty}{T_w - T_\infty}, \; \phi(\eta) = \frac{C - C_\infty}{C_w - C_\infty}, \; \eta = \frac{r^2 - a^2}{2a}\left(U_w/\nu_f x\right)^{\frac{1}{2}}. \tag{6}$$

In Eq. (6), ψ is the stream function defined as $u = \frac{1}{r}\psi_r$ and $\mathrm{v} = -\frac{1}{r}\psi_x$, which identically satisfies continuity Eq. (1). By defining η in the above form, the boundary condition at $r = a$ reduces to the boundary condition at $\eta = 0$, which is more convenient for analytical / numerical computations. Eqs. (2) - (4) with the help of (6) becomes :

$$\left((1+2\eta\gamma)f''\right)' - (f')^2 + ff'' + \lambda\theta + Gc\,\phi - Mn\,f' = 0, \tag{7}$$

$$\left((1+2\eta\gamma)\theta'\right)' - \Pr\left(f'\theta - f\theta'\right) + \Pr(1+2\eta\gamma)\left[Nb\;\theta'\varphi' + Nt\,\theta'^2\right] = 0, \tag{8}$$

$$\left((1+2\eta\gamma)\varphi'\right)' - Le\left(f'\phi - f\phi'\right) + \frac{Nt}{Nb}\left((1+2\eta\gamma)\theta'\right)' = 0, \tag{9}$$

The corresponding boundary conditions are :

$$f(0)=0,\quad f'(0)=1,\quad \theta(0)=1,\quad \phi(0)=1,$$
$$f'(\infty)=0,\quad \theta(\infty)=0,\quad \phi(\infty)=0. \tag{10}$$

Here, the parameters γ, K_1, λ, Gc, Nt, Nb, Pr and Le are the transverse curvature, the porous parameter, the buoyancy or free convection parameter, the mass Grashof number, the thermophoresis parameter, the Brownian motion parameter, the Prandtl number and the Lewis number which are defined as follows:

$$\gamma = \sqrt{\frac{\nu_f}{ba^2}},\ K_1 = \nu_f / K'b,\ \lambda = \pm\frac{g\beta T_0}{\rho_f b^2},\ Gc = \frac{g\beta^* C_0}{\rho_f b^2},\ Nt = \frac{\tau D_T\left(T_w - T_\infty\right)}{\nu_f T_\infty},$$
$$Nb = \frac{\tau D_B\left(C_w - C_\infty\right)}{\nu_f},\ \Pr = \frac{\nu_f}{\alpha} \text{ and } Le = \frac{\nu_f}{D_B}. \tag{11}$$

It is worth mentioning that $\lambda > 0$ aids the flow and $\lambda < 0$ opposes the flow, while $\lambda = 0$ i.e., $\left(T_w = T_\infty\right)$ represents the case of forced convection flow. On the other hand, if λ is of significantly greater order of magnitude than one, then the buoyancy forces will be predominant. Hence, combined convective flow exists when $\lambda = 0(1)$. For all practical purpose, the physical quantities of interest are the skin friction coefficient C_f, the local Nusselt number Nu_x and the local Sherwood number Sh_x, which are defined by:

$$\frac{1}{2}C_f\,\mathrm{Re}_x^{1/2} = f''(0),\ \frac{Nu_x}{\mathrm{Re}_x^{1/2}} = -\theta'(0) \text{ and } \frac{Sh_x}{\mathrm{Re}_x^{1/2}} = -\phi'(0), \tag{12}$$

where $\mathrm{Re}_x = U_w x/\nu_f$ is the local Reynolds number.

3. Exact solutions for some special cases when $\lambda = Gc = \gamma = 0$.

For $\lambda = Gc = \gamma = 0$, the convective flow, heat and mass transfer problem degenerates. In this case the closed form solution for the velocity field is given by

$$f = \frac{1 - e^{-m\eta}}{m} \text{ where } m = \sqrt{1+K_1}.$$

4. Numerical procedure

The Eqs. (7) - (9) are exceptionally non-linear, coupled ordinary differential equations with variable coefficients of third-order in f and second-order in both θ and ϕ solved by means of Keller-box technique. The coupled boundary value problem (7) - (9) has been lessened to a system of seven simultaneous ordinary differential equations of first order for three unknowns following the method of superposition. To solve the system of first order equations, seven initial conditions are required whilst only two initial conditions on f and one initial condition θ and ϕ are known. The solution process is repeated with larger value of η_∞ until two successive values of unknown conditions differ only after desired digit

signifying the limit of the boundary along η. The last value of η_∞ is chosen as appropriate value for that particular set of parameters. Finally, the problem is solved numerically using a second order finite difference scheme known as Keller-box method (See for details Vajravelu and Prasad [21]).

5. Results and discussion

In order to understand the mathematical nanofluid model, the numerical results are presented graphically for the axial velocity $f'(\eta)$, the temperature $\theta(\eta)$ and the species diffusion $\varphi(\eta)$ in Figs. 1-8 for different values of pertinent parameters. The computed numerical values for the skin friction $f''(0)$, the Nusselt number $\theta'(0)$ and the wall Sherwood number $\phi'(0)$ are tabulated in Table I.

Figures 1-2 are the graphical representation of $f'(\eta)$. It is obvious from Fig. 1 that the momentum boundary layer thickness is higher for $\gamma \neq 0$ as compared to $\gamma = 0$ and for increasing values of K_1 results in flattening of $f'(\eta)$. The transverse contraction of the velocity boundary layer is observed. The effect of flattening of axial velocity as a consequence of increasing the strength of the porous parameter is observed and it is true for all values of γ. The effect of increasing values of Gc and λ on $f'(\eta)$ is demonstrated in Fig. 2. Increase in Gc and λ leads to the enhancement of $f'(\eta)$. Under the supporting buoyancy condition, buoyancy acts a similar way to the approaching flow, in this manner really destabilizing the flow; while in the restricting buoyancy circumstance, buoyancy is acting inverse to the flow bearing, thereby suppressing flow instability. Under the cross-buoyancy circumstance, buoyancy collaborates with the flow in the cross-bearing. While the impact of aiding or opposing buoyancy on flow qualities might be foreseen from a physical point of view, the impact of cross-buoyancy on heat transport is difficult to foresee from the earlier. Furthermore, the state of the impediment and its introduction regarding the incoming flow affect the transport processes and the resulting wake dynamics. Physically, $\lambda < 0, \lambda > 0, \lambda = 0$ corresponds to an externally heated plate because the free convection currents are carried towards to the plate, corresponds to an externally cooled plate and corresponds to the absence of free convection currents. The behavior of $\theta(\eta)$ is recorded in Figs. 3 – 5. The effects of λ and K_1 on $\theta(\eta)$ are presented graphically in Fig. 3. An increase in the value of λ results in an increase in the thermal boundary layer thickness and this results in an increase in the magnitude of the wall temperature gradient and hence produces an increase in the surface heat transfer rate; this is even true for non-zero values of K_1. The effect of K_1 is to increase the wall temperature gradient and $\theta(\eta)$. *Nb* and *Nt* are two physical parameters of utmost interest, which depends on the type of the nanoparticle present through the parameters D_B and D_T, while Nb depends on the nanoparticle concentration namely $(C_w - C_\infty)$. An increase in either of the parameters *Nb* or *Nt* leads to decrease in the magnitude of the wall temperature gradient and hence, increases the thermal boundary layer thickness; exhibited graphically in Fig. 4. The effects of $\Pr$ and γ on $\theta(\eta)$ are depicted graphically in Fig. 5. It is clear from the graph that an increase in $\Pr$ leads to decrease the temperature distribution and hence thermal boundary layer thickness. The effect of increasing values of γ is to increase the temperature and hence enhances the thermal boundary layer thickness.

Figs. 6 – 8 explain the effects of different parameters on $\varphi(\eta)$. Fig.6 illustrates the effects of K_1 and *Gc* on $\varphi(\eta)$. It is noticed that the effect of K_1 and *Gc* is to enhance $\varphi(\eta)$. The

effect of Nb and Nt on $\varphi(\eta)$ is shown in Fig. 7. It can be seen that $\varphi(\eta)$ increases with an increase in Nb as well as Nt. The effect of increasing values of Le leads to decrease in the thickness of the nanoparticle concentration boundary layer which is ahown in Fig.8. This is due to the thinning of the nanoparticle layer with the introduction of species diffusion. This phenomenon is true even for increasing values of γ.

From Table I it is clear that $f''(0)$, $\theta'(0)$ and $\phi'(0)$ found to decrease with increase in γ. An increase in λ leads to an increase in $f''(0)$ and decrease in $\theta'(0)$ and $\phi'(0)$, but the reverse trend is found in K_1. It is interesting to note that the surface mass transfer decreases and surface heat transfer increases with Le, Nb and Nt.But the effect of $\Pr$ is to decrease $\theta'(0)$ and increase $\phi'(0)$.

6. Conclusion

The following conclusions are drawn from the computed numerical values. The considerable increment the heat transfer rate at any given buoyancy parameter is because of suspended nanoparticle and similar trend is continued with respect to Brownian movement parameter and the thermophoresis parameter, Grashof number for the thermal and as well as nanoparticle concentration profiles respectively. The opposite behavior is recorded for Lewis number. Skin-friction increases for increasing values of mass Grashof number and thermophoresis parameter. However opposite effect is observed for Brownian motion parameter and Lewis number. Sherwood number enhance for larger values of porous parameter and Prandtl number the reverse trend is observed in the case of Brownian motion parameter, the thermophoresis parameter and the Lewis number.

References

1. S. Choi, Enhancing thermal conductivity of fluids with nanoparticle. In: D.A. Siginer, H.P. Wang (Eds.), Developments and Applications of Non- Newtonian Flows, ASME, MD 231 and FED 66 (1995) 99-105.
2. J. Buongiorno, Convective Transport in Nano Fluids, Journal of Heat and Transfer, ASME 128 (2006) 240−250.
3. Shehzada, N., Zeeshana, A., Ellahiab, R., Vafaib, K. (2016), “Convective heat transfer of nanofluid in a wavy channel: Buongiorno's mathematical model”, J. Mol. Liq. Vol. 222, 446-455.
4. M. Sheikholeslami, D.D. Ganji, M.M. Rashidi, Magnetic field effect on unsteady nanofluid flow and heat transfer using Buongiorno model, J. Magnetism and Magnetic Materials, 2015, Vol. 416(15),164-173.
5. Prasad, K.V., Vajravelu, K, Vaidya, H , MHD Casson Nanofluid Flow and Heat Transfer at a Stretching Sheet with Variable Thickness, Journal of Nanofluids, Vol.5, (3), 2016, pp. 423-435(13).
6. K. Vajravelu1, K. V. Prasad, Hanumesh Vaidya, Influence of Hall Current on MHD Flow and Heat Transfer over a slender stretching sheet in the presence of variable fluid properties, Communications in Numerical Analysis 2016 No.1 (2016) 17-36
7. C.Y. Wang, Fluid flow due to a stretching cylinder, Phys. Fluids **31** (1988) 466-468.
8. A. Ishak, R. Nazar, Laminar boundary layer flow along a stretching cylinder, Euro. J. Sci. Res. 36 (2009) 22–29.
9. N. Bachok, A. Ishak, Flow and heat transfer over a stretching cylinder with prescribed surface heat flux, Malaysian J. of Math. Sci. 4 (2010) 159-169.
10. A.J. Chamkha, M.M. Abd El-Aziz, S.E. Ahmed, Effects of thermal stratification on flow and heat transfer due to a stretching cylinder with uniform suction/injection, Int. J. Energy & Technology 2 (2010) 1-7.

11. A. Ishak, Similarity Solutions for flow and heat transfer over a permeable surface with convective boundary condition, Applied Mathematics and Computation, 217 (2010) 837–842.
12. K.V. Prasad, K. Vajravelu, Hanumesh Vaidya, B. T. Raju, Heat Transfer in a Non-Newtonian Nanofluid Film Over a Stretching Surface. Journal of Nanofluid 4 (2015) 1-12.
13. K. Vajravelu, K.V. Prasad, S.R. Santhi, Axisymmetric magneto-hydrodynamic (MHD) flow and heat transfer at a non-isothermal stretching cylinder, Applied Mathematics and Computation 219 (2012) 3993-4005.
14. T. Mahmood, J.H. Merkin, Similarity solutions in axisymmetric mixed-convection boundary-layer flow, J. Eng. Math. 22 (1988) 73-92.
15. P. Ganesan, P. Loganathan, Numerical study of double-duffusive, free convective flow past moving vertical cylinder with chemically reactive species diffusion, J. Eng. Phys. Thermo Phys. 79 (2006) 73–78.
16. N. Bachok, A. Ishak, Mixed convection boundary layer flow over a permeable vertical cylinder with prescribed surface heat flux, Euro. J. of Sci. Res. 34 (2009) 46–54.
17. Rani, H. & Devaraj, R , Numerical solution of unsteady flow past a vertical cylinder with temperature oscillations, Forsch Ingenieurwes (2003) 68: 75. https://doi.org/10.1007/s10010-003-0108-5.
18. K. Vajravelu, Convection heat transfer at a stretching sheet with suction or blowing, J. Math. Anal. Anal. 188 (1994) 1002–1011.
19. K. Vajravelu and K.V. Prasad, Keller-box method and its application (HEP and Walter De Gruyter GmbH, Berlin/Boston, 2014).
20. Prasad, K. V.; Vajravelu, K.; Vaidya, Hanumesh; Santhi, S. R., Axisymmetric Flow of a Nanofluid Past a Vertical Slender Cylinder in the Presence of a Transverse Magnetic Field, Journal of Nanofluids, Vol. 5(1)2016, pp. 101-109(9).

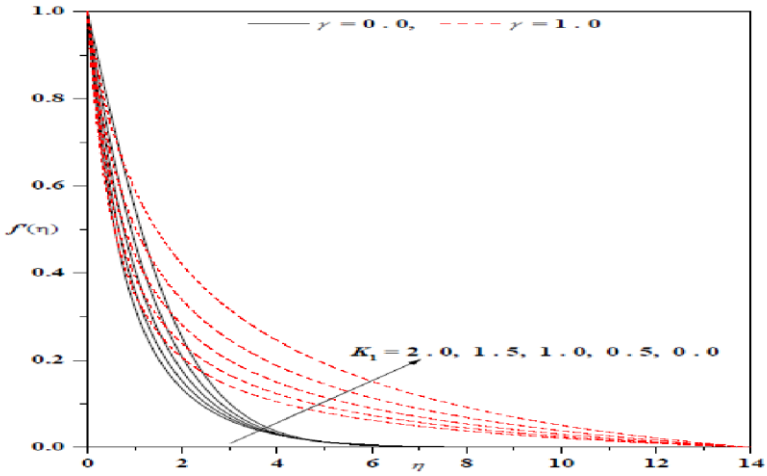

Fig . 1 : Axial Velocity profiles for different values of K_1 and γ

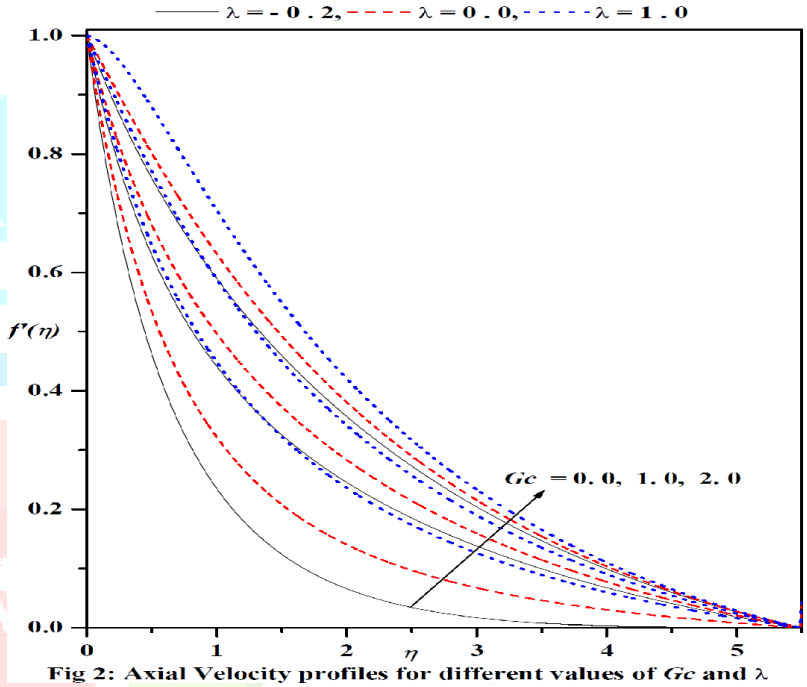

Fig 2: Axial Velocity profiles for different values of Gc and λ

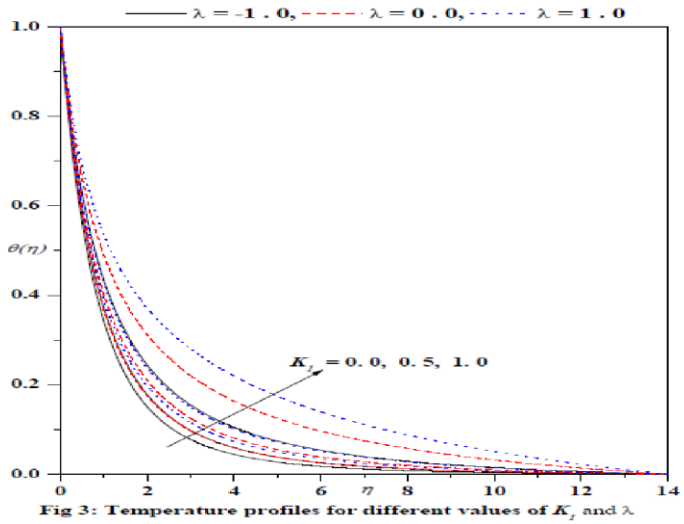

Fig 3: Temperature profiles for different values of K_1 and λ

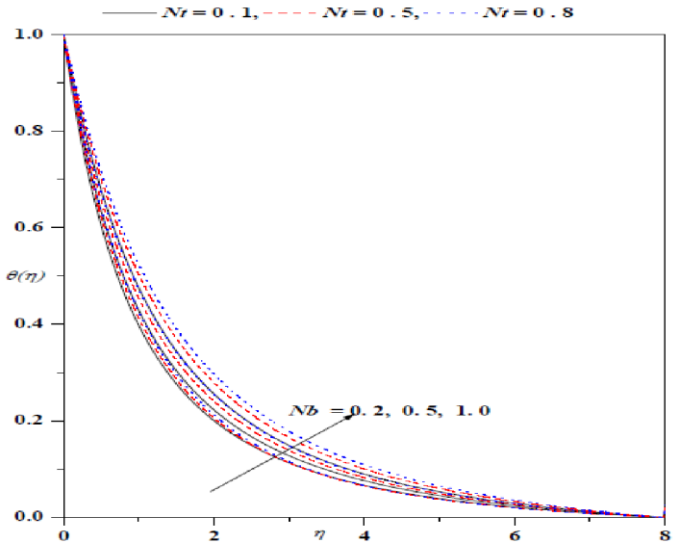

Fig 4: Temperature profiles for different values of Nt and Nb

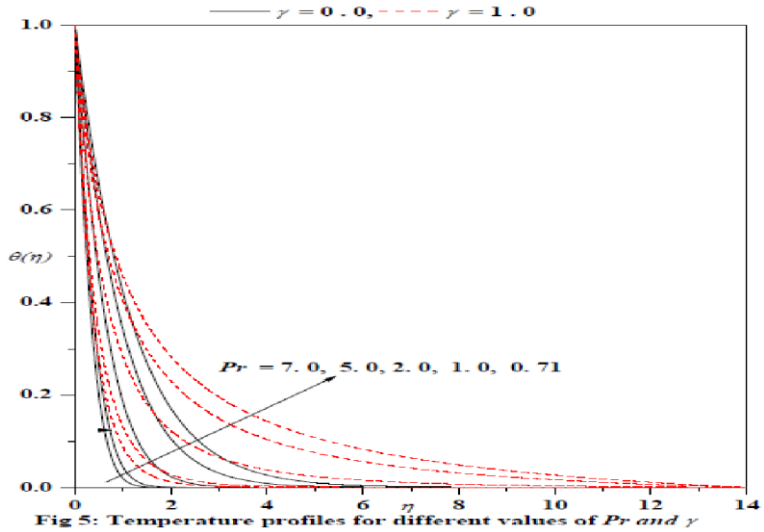

Fig 5: Temperature profiles for different values of *Pr and* γ

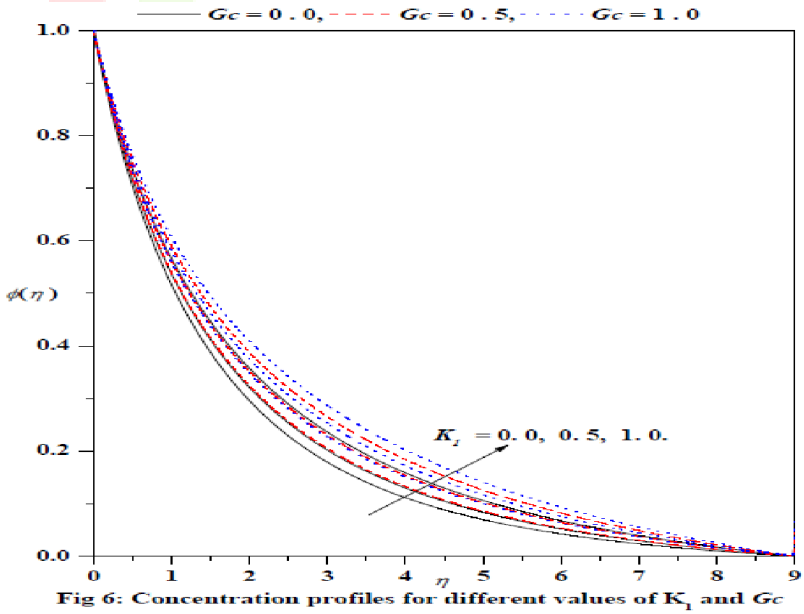

Fig 6: Concentration profiles for different values of K_1 and *Gc*

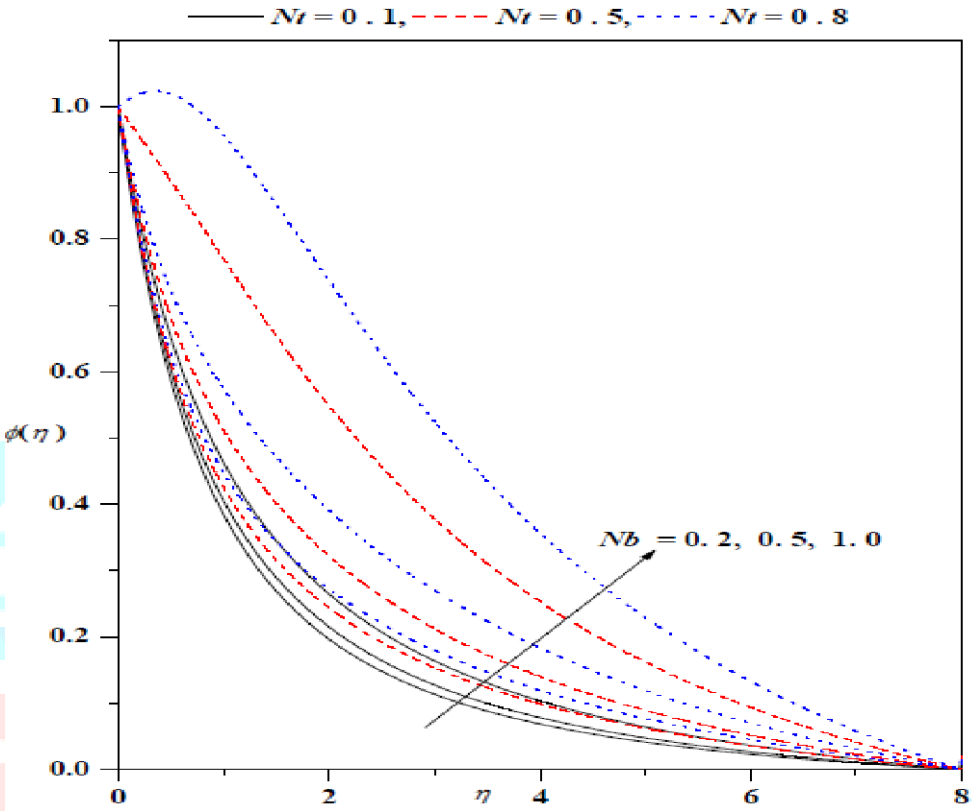

Fig 7: Concentration profiles for different values of Nt and Nb

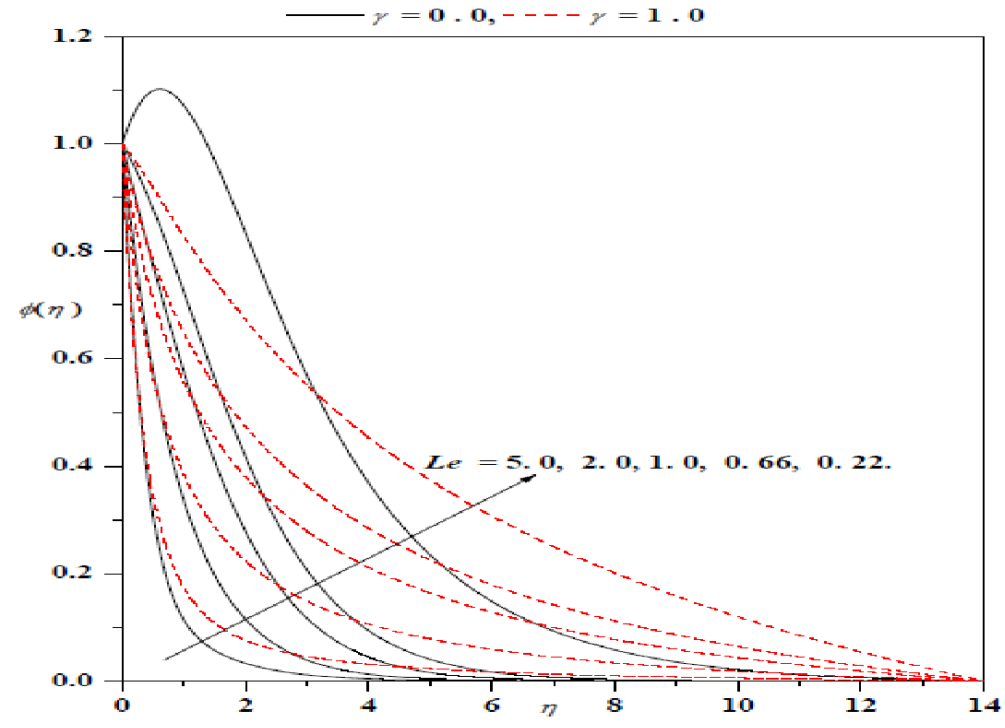

Fig 8: Concentration profiles for different values of Le and γ

Table I: Numerical values of skin friction, wall temperature gradient and mass concentration gradient for different values of the pertinent parameter

Le	Pr	Nt	Nb	λ	Gc	K_1	$\gamma = 0.0$			$\gamma = 1.0$		
							$-f''(0)$	$-\theta'(0)$	$-\phi'(0)$	$-f''(0)$	$-\theta'(0)$	$-\phi'(0)$
1.0	1.0	0.1	0.1	0.5	0.5	0.0	0.488382	1.044617	0.488382	0.7630559	1.381393	0.763056
						0.5	0.730834	1.003362	0.480790	1.053078	1.328420	0.879580
						1.0	0.941974	0.966951	0.444436	1.295051	1.283998	0.843786
						2.0	1.300339	0.905127	0.385932	1.690290	1.213252	0.794390
			0.1									
		1.0	0.1									
1.0												
1.0	1.0	0.1	0.1	0.5	0.0	0.5	0.995219	0.945957	0.415310	1.346942	1.265400	0.827119
					0.5		0.730834	1.003362	0.480790	1.053078	1.328420	0.879580
					1.0		0.490730	1.043772	0.521846	0.784078	1.375145	0.919847
					2.0		0.049224	1.104255	0.578939	0.292282	1.444810	0.980368
						0.5						
1.0	1.0	0.1	0.1	-1.0	0.5	0.5	1.387258	0.873580	0.353948	1.864274	1.131488	0.738381
				0.0			0.931613	0.971772	0.451797	1.285650	1.288342	0.848186
				1.0			0.539836	1.030059	0.504600	0.835132	1.361002	0.905409
					0.5							
1.0	1.0	0.5	0.1	0.5	0.5	0.5	0.5278722	0.966843	-1.41229	0.868217	1.225685	-0.56263
			0.2				0.648645	0.907029	-0.12116	0.993196	1.148852	0.542179
			0.5				0.722239	0.796869	0.650743	1.060483	0.998946	1.182603
			0.8				0.736879	0.710969	0.840947	1.069640	0.8782179	1..334056
			1.0				0.739801	0.660465	0.903008	1.069690	0.806899	1.381743
1.0	1.0	0.1	0.1	0.5	0.5	0.5	0.791160	0.968181	1.042115	1.115520	1.294431	1.403890
		0.2					0.788799	0.935491	1.042907	1.111970	1.246000	1.404993
		0.5	0.1				0.781915	0.849373	1.045284	1.101469	1.118591	1.408336
		0.8					0.775345	0.778274	1.047645	1.091254	1.013689	1.411707
		1.0					0.771147	0.737675	1.049202	1.084633	0.953961	1.413952
1.0	0.71	0.1	0.1	0.5	0.5	0.5	0.718799	0.831519	0.614266	1.044402	1.168213	1.006694
	1.0						0.730834	1.003362	0.480790	1.053078	1.328420	0.879580
	2.0						0.751619	1.438164	0.128425	1.071466	1.735197	0.548287
	5.0						0.770660	2.207656	-0.53438	1.091964	2.419522	-0.00344
	7.0						0.775508	2.544959	-0.83604	1.097521	2.699775	-0.28070
0.22	1.0	0.1	0.1	0.5	0.5	0.5	0.591857	1.082823	-0.35674	0.942272	1.388134	0.120878
0.66							0.691326	1.026605	0.191203	1.016340	1.348361	0.601865
1.0							0.730834	1.003362	0.480790	1.053078	1.328420	0.879580
2.0							0.792864	0.967461	1.097680	1.118585	1.292956	1.489609
5.0							0.859866	0.931789	2.253599	1.196602	1.252187	2.649752

nclature

a radius of the cylinder
b stretching rate
C concentration of the fluid
C_f skin friction coefficient
C_w concentration of the stretching sheet
K' the permeability of the porous medium
C_0 constant
C_∞ concentration of the fluid for away from the wall
c_f specific heat of the fluid
c_p specific heat of the nano particle (J/kg · K)
D mass diffusivity
D_B Brownian diffusion coefficient
D_T thermophoretic diffusion coefficient
f dimensionless stream function
g acceleration due to gravity
Gc mass Grashof number
K_1 permeability parameter
k thermal conductivity (W/m · K) W m^{-1} K^{-1}
l reference length
Le Lewis number
Nb Brownian motion parameter
Nt thermophoresis parameter
Nu_x local Nusselt number
Pr Prandtl number
q_m surface mass flux
q_w surface heat flux
r radial coordinate
Re_x local Reynolds number
Shx local Sherwood number
T fluid temperature (K)
T_w temperature of the stretching sheet (K)
T_∞ ambient temperature(K)
T_0 constant (K)
u axial velocity component (m^2/s)
U_w stretching velocity(m/s)
v radial velocity component
x axial coordinate

Greek symbols

α thermal diffusivity
β thermal expansion coefficient
β^* concentration expansion coefficient
γ transverse curvature
η similarity variable
θ dimensionless temperature
φ dimensionless concentration
ψ stream function
μ dynamic viscosity(Pa.s)
ν_f kinematic viscosity of the fluid(m^2/s)
ρ_f density of the fluid (kg/m^3)
ρ_p density of the nanoparticle (kg/m^3)
$(\rho c)_f$ heat capacity of the fluid ($kg/m^3 \cdot K$)
$(\rho c)_p$ effective heat capacity of the nanoparticle material ($kg/m^3 \cdot K$)
λ free convection parameter
$\tau = (\rho c)_p / (\rho c)_f$ ratio between the effective heat capacity of the nanoparticle material and heat capacity of the fluid
τ_w surface shear stress (kg m^{-1} s^{-2})

Subscript

w conditions at the stretching sheet
∞ condition at infinity

Superscript

‘ differentiation with respect to η